Successive Multipath Interference Cancellation for CP-Free OFDM Systems

Xiqing Liu, Hsiao-Hwa Chen, *Fellow, IEEE*, Weixiao Meng, *Senior Member, IEEE*, and Bo-Yu Lyu

***Abstract*—Traditional orthogonal frequency-division multiplexing (OFDM) systems mitigate multipath interferences with the help of a cyclic prefix (CP) appended between two adjacent OFDM blocks. The length of the CP must be made longer than channel delay spread to avoid intersymbol interference (ISI). The use of CPs degrades spectrum efficiency significantly, which is a deal price paid in all existing OFDM systems. Motivated to deal with this issue, this paper proposes a CP-free OFDM scheme with successive multipath interference cancellation (SMIC), which does not require CPs and removes ISI before fast Fourier transform (FFT) at a receiver using stored feedback equalization (SFE). The SFE operation leaves a CP gap between adjacent OFDM blocks, and the CP is regenerated with estimated signals. In this way, we convert linearly shifted OFDM blocks induced by multipath propagation back to cyclically shifted OFDM blocks for successful FFT operation. SMIC-OFDM achieves a much higher spectrum efficiency than traditional OFDM owing to the save of CPs in transmission signals. The performance of SMIC-OFDM in terms of the bit error rate, capacity, and computational complexity is compared to that of traditional OFDM to verify the effectiveness of the proposed SMIC-OFDM scheme.**

***Index Terms*—Cyclic prefix (CP), spectrum efficiency, stored feedback equalization (SFE), successive multipath interference cancellation (SMIC).**

I. Introduction

ORTHOGONAL frequency-division multiplexing (OFDM) and orthogonal frequency-division multiple-access (OFDMA) techniques have been widely used in digital audio broadcasting, digital video broadcasting, IEEE 802.11 (WLAN), IEEE 802.16 (WiMax), and the fourth-generation wireless communication systems [1]. In a multipath scenario, a receiver may observe a train of signals from the same source, and the sum of their delayed replicas creates multipath-induced intersymbol interference (ISI). Thus, a cyclic prefix (CP) has to be appended to each OFDM block at a transmitter to avoid ISI and intercarrier interference (ICI) [2]. The CP should be removed before fast Fourier transform (FFT) at a receiver. The CP, as its name implies, creates transmission overhead, which is a duplicated copy of the tail of an OFDM block. Via CP insertion in each OFDM block, the bandwidth of each subcarrier becomes narrower than the coherence bandwidth, and thus, user data in a block can be protected by the CP from frequency-selective fading [3]. Unfortunately, CP insertion in an OFDM block impairs spectrum efficiency. In some applications, spectral loss because of the CP can go up to 25%, which is a significant loss [5]. Moreover, in future wireless communications with a higher data rate to support latency-sensitive applications, this problem will become even worse [6].

Since the length of a CP is decided mainly by the length of channel impulse response (CIR), many works investigated CIR shortening techniques as an effort to reduce the CP [7], [9]–[11]. The third-generation partnership project long-term evolution (3GPP-LTE) standard defines two types of CPs, namely normal CP and extended CP, whose lengths are 7.04% and 25% of a block length, respectively. In [10], Kim *et al.* pointed out that the extended CP causes a too heavy loss in spectrum efficiency and suggested to use the normal CP-only strategy plus a CIR shortening algorithm in an OFDMA downlink scenario. Their proposed scheme, based on a minimum subband interference criterion, takes care of only the nulls within the subcarriers of interest and, thus, can achieve more degrees of freedom. In [7], Park and Im proposed an ISI/ICI elimination scheme for the cases that the CP length is shorter than the delay spread. The proposed scheme dealt with ISI and ICI separately at the transmitter and the receiver, respectively. In [9], a decision-aided interference cancellation algorithm was proposed to eliminate residual ISI introduced by the delay spread that exceeds the CP length. The proposed scheme can be applied to all types of channels. An iteration algorithm called residual intersymbol interference cancellation (RISIC) based on tail cancellation and CP reconstruction was suggested in [8]. It offers an acceptable performance only if the length of the delay spread is moderate. In addition, several turbo equalization algorithms based on tail cancellation and CP reconstruction were proposed. In [12], a low-complexity turbo frequency-domain equalization (Turbo-FDE) scheme characterized by soft cancellation followed by the minimum mean-squared-error algorithm was investigated for the scenarios with an insufficient CP. In [13], a Turbo-FDE technique was developed to suppress ISI/ICI for CP-free block transmission, which was named as chained turbo equalization, in

Manuscript received September 4, 2017; revised February 5, 2018 and April 25, 2018; accepted May 15, 2018. This work was supported in part by the National Natural Science Foundation of China under Grant U1764263, Grant 61671186, and Grant 91438205, and in part by the Taiwan Ministry of Science and Technology under Grant 106-2221-E-006-021-MY3, Grant 106-2221-E-006-028-MY3, and Grant 107-2811-E-006-004. *(Corresponding author: Hsiao-Hwa Chen.)*

X. Liu and H.-H. Chen are with the Department of Engineering Science, National Cheng Kung University, Tainan 7010, Taiwan (e-mail: hstsliou@gmail.com; hshwchen@ieee.org).

W. Meng is with the Communication Research Center, Harbin Institute of Technology, Harbin 150001, China (e-mail: wxmeng@hit.edu.cn).

B.-Y. Lyu is with the Virginia Polytechnic Institute and State University, Blacksburg, VA 24061 USA (e-mail: boyu93@vt.edu).

Digital Object Identifier 10.1109/JSYST.2018.2838663

which data blocks at a receiver can be recovered by exchanging *a posteriori* information of the overlapping components. In the proposed Turbo-FDE, bit-error-rate (BER) performance relies very much on another type of redundancy, e.g., a 1/2 rate convolutional coding scheme [14]. Moreover, in tail cancellation operation, the previous OFDM symbol was assumed to be detectable without any error, and thus, the ISI term can be canceled completely. Nevertheless, it was a bit too ideal assumption.

In our earlier research efforts [15], [16], we proposed a CP-free OFDM scheme, which was called symbol cyclic shift equalization (SCSE). To implement SCSE, decision feedback equalization (DFE) must be used before the CP restoration/regeneration (CPR) algorithm for ISI elimination. However, the use of DFE has three drawbacks. First, when a symbol is decoded with an error, the feedback signal will not be real ISI, resulting in feedback errors, which will propagate to the detection of the following blocks [19]–[21]. Second, to reconstruct the ISI component, an inverse fast Fourier transform (IFFT) and a convolution operation are required for feedback signal processing, which leads to a high computational complexity. Third, DFE used therein is very sensitive to feedback delay, since the ISI must be subtracted immediately before the upcoming CPR [22], [23]. If channel coding is employed, the decoding delay may become even longer. For detection of the current OFDM block, if the feedback signal cannot be acquired in time, a detection interruption will occur, which affects the robustness of the system. To address this issue, this work utilizes stored feedback equalization (SFE) instead of DFE to remove ISI. The computational complexity is lower, and the feedback loop is much shorter than DFE.

The rest of this paper can be outlined as follows. In Section II, the system structure of SMIC-OFDM will be presented, and its block diagram will be given. In Section III, the SMIC algorithm will be introduced, and the implementation issues will be discussed. The simulation results will be given, and performance comparisons among different schemes will be made in Section IV, followed by the conclusion of this paper in Section V.

II. System Model

In this section, the block diagrams of an SMIC-OFDM system are presented, including the transmitter and the receiver along with the definitions of variables used in this paper.[1]

The ith data block is assumed to be the signal of interest. As shown in Fig. 1, a mapper maps binary inputs $\mathbf{b}_i^T = [b_{i,0}, \ldots, b_{i,K-1}]$ into a block of $\mathcal{M}$-ary modulated symbols $\mathbf{q}_i^T = [q_{i,0}, \ldots, q_{i,M-1}]$. Here, the modulation can be quadrature amplitude modulation (QAM), phase-shift-keying modulation, pulse amplitude modulation (PAM), and so on. Assume that the modulation level is $\mathcal{M} = 2^{K/M}$, where K and M refer to the lengths of binary bits and data block, respectively. Then, $\mathbf{q}_i^T$ is sent into a serial-to-parallel (S/P) converter before the IFFT module, yielding $\mathbf{q}_i$. Thereafter, an M-point IFFT is

[1]Particularly, "$\mathbf{x} = [x_0, \ldots, x_{A-1}]^T = [x_a]_{a=0}^{A-1}$" is used in this paper to denote a column vector with dimension of A, and "$\mathbf{x}^T = [x_0, \ldots, x_{A-1}]$" denotes the corresponding row vector, unless otherwise stated.

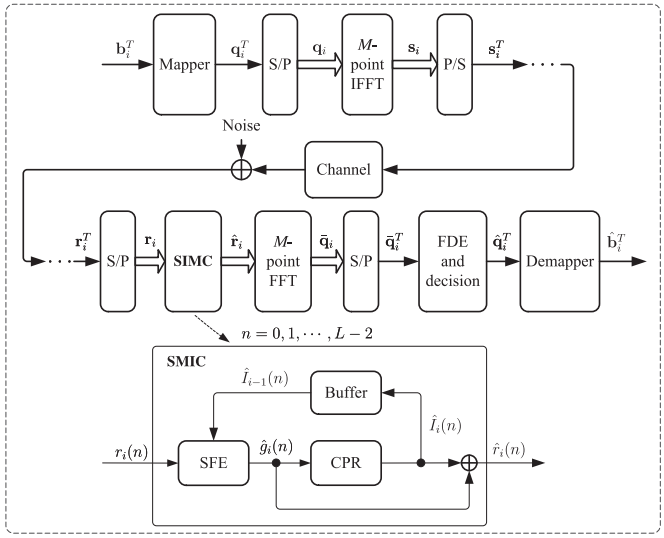

Fig. 1. Block diagram of the SMIC-OFDM system including its transmitter and receiver. In the transmitter, a binary bit sequence is mapped into a block of modulated symbols, and then, it will be sent into S/P, IFFT, and P/S, respectively. After a multipath channel, a received OFDM block will go through S/P and be processed by the SMIC module before FFT. After FFT and P/S, a SMIC-OFDM block will be sent into FDE and a decision device. Finally, the recovered block will be translated into binary bits by a demapper.

performed on $\mathbf{q}_i$ to generate an OFDM block, or

$$\mathbf{s}_i = \mathbf{F}^{-1}\mathbf{q}_i = \left[s_i(0), \ldots, s_i(M-1)\right]^T \tag{1}$$

where $\mathbf{F}^{-1}$ is an IFFT matrix with its size as $M \times M$, and it can be written as

$$\mathbf{F}^{-1} = \frac{1}{\sqrt{M}} \begin{bmatrix} 1 & 1 & \cdots & 1 \\ 1 & W_M & \cdots & W_M^{(M-1)} \\ \vdots & \vdots & \ddots & \vdots \\ 1 & W_M^{(M-1)} & \cdots & W_M^{(M-1)(M-1)} \end{bmatrix}^{-1} \tag{2}$$

in which W_M is equal to $e^{-j2\pi/M}$ and "$[\cdot]^{-1}$" stands for matrix inversion. After IFFT and P/S conversion, $\mathbf{s}_i$ will be sent into a wireless channel.

Let us consider a discrete baseband multipath channel model [25], [26]. We define $h(l) = \rho_l e^{2\pi\phi_l}$ as the complex gain of path l $(l = 0, \ldots, L-1)$, where ρ_l follows a Rayleigh distribution and $e^{2\pi\phi_l}$ obeys a uniform distribution in $[0, 2\pi]$. The delay spread is $L-1$, which is assumed to be shorter than the length of an OFDM block, namely $L - 1 < M$. The multipath channel matrix can be written as

$$\mathbf{H} = \begin{bmatrix} h(0) & 0 & \cdots & \cdots & \cdots & 0 \\ \vdots & \ddots & \ddots & & & \vdots \\ h(L-1) & & \ddots & \ddots & & \vdots \\ 0 & \ddots & & \ddots & \ddots & \vdots \\ \vdots & \ddots & \ddots & & \ddots & 0 \\ 0 & \cdots & 0 & h(L-1) & \cdots & h(0) \end{bmatrix}_{M \times M}. \tag{3}$$

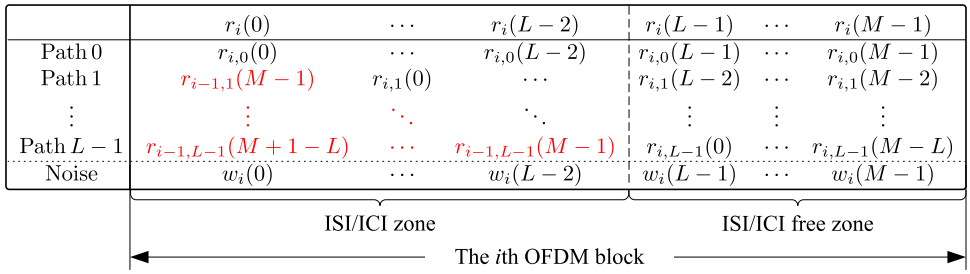

Fig. 2. Illustration of the received block of interest, which is partitioned into ISI/ICI and ISI/ICI free zones. The length of the ISI/ICI zone is equal to the delay spread of the channel. In the ISI/ICI zone, the interferences are marked in red.

After going through a multipath channel, the ith block of the received signal $\mathbf{r}_i$ consists of an ISI term ($\mathbf{I}_{i-1}$), which is created by multipath returns of the previous block, i.e., the $(i-1)$th block, or

$$\begin{aligned}\mathbf{r}_i &= \left[r_i(n)\right]_{n=0}^{M-1} = \mathbf{H}\mathbf{s}_i + \mathbf{I}_{i-1} + \mathbf{w}_i \\ &= \left[g_i(n)\right]_{n=0}^{M-1} + \left[I_{i-1}(n)\right]_{n=0}^{M-1} + \left[w_i(n)\right]_{n=0}^{M-1} \end{aligned} \tag{4}$$

where $\mathbf{w}_i = [w_i(n)]_{n=0}^{M-1}$ refers to an additive white Gaussian noise term. Perform the SMIC algorithm, including SFE and CPR, on $\mathbf{r}_i$ before FFT. Specifically, SFE is implemented first to suppress ISI, yielding $[\hat{g}_i(n)]_{n=0}^{L-2}$, and then, CPR reconstructs the block by calculation of $\hat{I}_i(n)$, or

$$\hat{\mathbf{r}}_i = \left\{ \left[\hat{g}_i(n) + \hat{I}_i(n)\right]_{n=0}^{L-2};\ \left[g_i(n)\right]_{n=L-1}^{M-1} \right\}. \tag{5}$$

After SMIC operation, a newly constructed block will be sent into FFT and P/S to yield $\bar{\mathbf{q}}_i$ and $\bar{\mathbf{q}}_i^T$, respectively. It can be shown that $\hat{\mathbf{r}}_i$ is a summation of different circularly shifted OFDM blocks plus noise, and thus, a one-tap frequency-domain filter needs to be applied to $\bar{\mathbf{q}}_i^T$ for removing random phases before the decision device. After making decision, a demapper translates the recovered data block $\hat{\mathbf{q}}_i^T$ into recovered binary bits $\hat{\mathbf{b}}_i^T$. Thus far, we have introduced the system model of SMIC-OFDM, and in Section III, we will show that with the help of the SMIC algorithm, a CP-free OFDM block can survive ISI/ICI induced by multipath propagation.

III. Successive Multipath Interference Cancellation

As discussed in Section II, the delay spread is assumed to be shorter than the length of a CP-free OFDM block. Hence, as shown in Fig. 2, in the current block (i.e., the ith block), only partial samples suffer from ISI/ICI, and the segment in which ISI/ICI occurs is called the ISI/ICI zone, whose length is $L-1$. Thus, (4) can be written as

$$\mathbf{r}_i = \left\{ \underbrace{\left[g_i(n) + I_{i-1}(n) + w_i(n)\right]_{n=0}^{L-2}}_{\text{ISI/ICI zone}};\ \underbrace{\left[g_i(n) + w_i(n)\right]_{n=L-1}^{M-1}}_{\text{ISI/ICI free zone}} \right\} \tag{6}$$

in which $g_i(n)$ can be further expressed as

$$g_i(n) = \begin{cases} \sum_{l=0}^{n} r_{i,l}(n-l), & n = 0, \ldots, L-2 \\ \sum_{l=0}^{L-1} r_{i,l}(n-l), & n = L-1, \ldots, M-1 \end{cases} \tag{7}$$

where $r_{i,l}(n-l)$ stands for the $(n-l)$th symbol in the ith block of path l. As shown in Fig. 3, SFE is performed on the samples affected by ISI/ICI, yielding

$$\left[\hat{g}_i(n)\right]_{n=0}^{L-2} = \left[r_i(n)\right]_{n=0}^{L-2} - \left[\hat{I}_{i-1}(n)\right]_{n=0}^{L-2}. \tag{8}$$

Assume that the calculation of $[\hat{I}_{i-1}(n)]_{n=0}^{L-2}$ has been done in the previous [i.e., the $(i-1)$th] block and saved in a buffer serving as a feedback signal. This operation is named as SFE. SFE is used here for suppressing the ISI term, which consists of multipath returns of the previous block.[2] The ISI in a CP-free OFDM block can be removed through feedback equalization, leaving a CP "gap," as discussed in our earlier work [15], [16]. This CP "gap" can be viewed as the sum of different linearly shifted versions of an OFDM block due to multipath propagation. In fact, FFT/IFFT is an algorithm based on a periodic signal, and a cyclic shift in the time/frequency domain can be considered as a phase rotation in the frequency/time domain in FFT/IFFT operation, while a linear shift in the time/frequency domain will bring in distortion to a signal if this signal is transformed into the frequency/time domain via FFT/IFFT [24]. In an OFDM system, sending a block of linearly shifted OFDM symbols into FFT will result in the interferences between subcarriers, which is called ICI [17]. To suppress ICI, we have to regenerate the CP via signal estimation, and this operation is called CPR. Before CPR, SFE is required to be done first. As shown in Fig. 3, $\hat{g}_i(n)$ $(n = 0, \ldots, L-2)$ is the input to CPR, which has been processed by SFE. The nth symbol experiencing path l can be estimated as

$$\left[\hat{r}_{i,l}(n)\right]_{l=0}^{L-1} = \left[\hat{g}_i(n) - \hat{D}_i(n)\right] \frac{\left[h(l)\right]_{l=0}^{L-1}}{h(0)} \tag{9}$$

in which $\hat{D}_i(n)$ is an intermediate term, and $[\hat{r}_{i,l}(n)]_{l=0}^{L-1}$ will be sent to a memory. When we implement (9) on the nth sample, the calculation of $\hat{D}_i(n)$ should already be done, as it contains the

[2]If an OFDM block is preceded by an idle period, whose length is at least equal to the delay spread, this OFDM block will not suffer from ISI and thus SFE can be skipped in detection of this block. However, the CPR is still necessary owing to the fact that a linearly shifted OFDM block must be converted into a circularly shifted one for successful FFT operation followed.

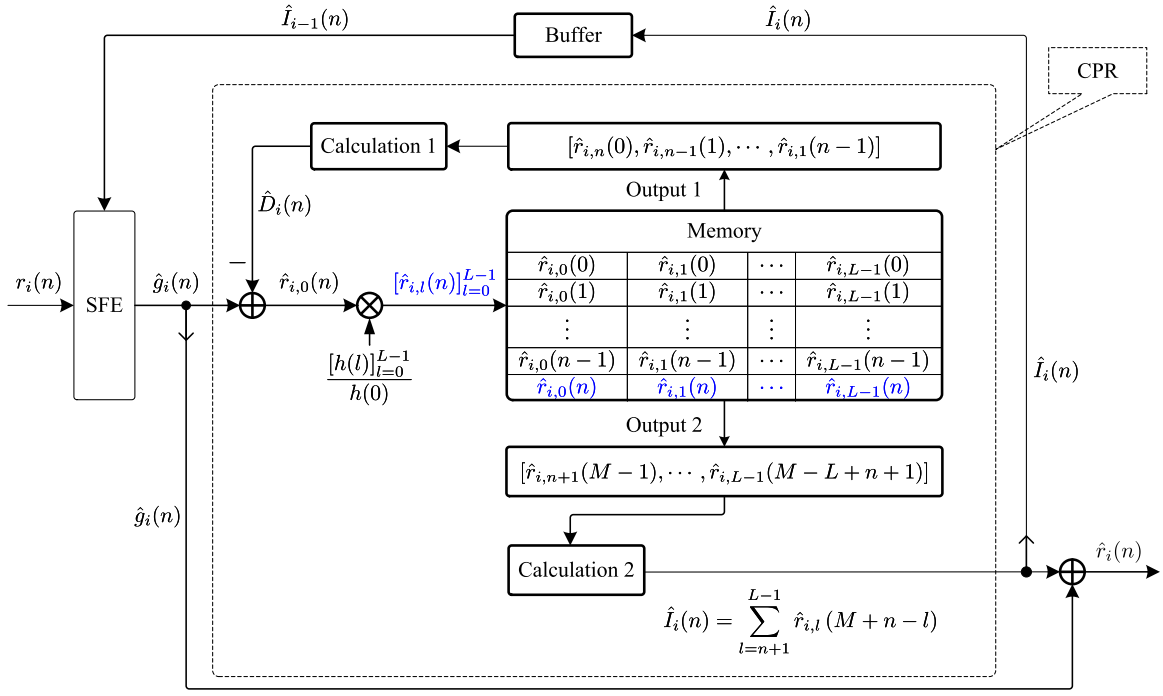

Fig. 3. Block diagram of the SMIC algorithm, where $r_i(n)$ is the nth sample in the ith SMIC-OFDM block, and $n = 0, 1, \ldots, L-2$. $\hat{I}_{i-1}(n)$ is the feedback signal, denoting the interference from the $(i-1)$th SMIC-OFDM block. $\hat{D}_i(n)$ is an intermediate variable in CPR operation, as defined in (10).

previous symbols, that is, $\hat{r}_{i,l}(0), \ldots, \hat{r}_{i,l}(n-1)$. The operation to calculate $\hat{D}_i(n)$ is denoted as "Calculation 1" in Fig. 3, and mathematically, $\hat{D}_i(n)$ can be written as

$$\hat{D}_i(n) = \begin{cases} 0, & n = 0 \\ \sum_{l=1}^{n} \hat{r}_{i,l}(n-l), & 1 \le n \le L-2. \end{cases} \tag{10}$$

As shown in Fig. 3, $\hat{I}_i(n)$ is the estimation of the CP signal, and (9) and (10) can provide sufficient information to calculate $\hat{I}_i(n)$ or perform "Calculation 2," which is expressed by

$$\hat{I}_i(n) = \sum_{l=n+1}^{L-1} \hat{r}_{i,l}\,(M+n-l)\,, \quad 0 \le n \le L-2. \tag{11}$$

Fig. 4 illustrates an example to explain the CPR in detail, where an OFDM block contains eight samples. A three-ray channel model is considered here, whose interpath delay is assumed to be one symbol time. "ⓝ" denotes the nth symbol in an OFDM block. According to Fig. 4, the CPR algorithm proceeds in eight steps. The noise term is temporarily excluded from the derivation for simplicity. Next, we illustrate the operation step by step.

1) *Step 1:* Multiply the first sample by the channel impulse response vector (CIRV), from which we can detect the first symbol from path $l\,(l = 0, 1, 2)$, or $\hat{g}_i(0)\frac{\mathbf{h}}{h(0)} = \left[\hat{r}_{i,l}(0)\right]_{l=0}^{2}$. Subtracting the second sample from the first symbol of path 1, we get the second symbol in path 0, or $[\hat{g}_i(1) - \hat{r}_{i,1}(0)] = \hat{r}_{i,0}(1)$.
2) *Step 2:* Multiplying $\hat{r}_{i,0}(1)$ acquired in Step 1 yet again by the CIRV, we can get the second symbols from paths 0, 1, and 2, or $\hat{r}_{i,0}(1)\frac{\mathbf{h}}{h(0)} = \left[\hat{r}_{i,l}(1)\right]_{l=0}^{2}$. Having acquired $\hat{r}_{i,2}(0)$ and $\hat{r}_{i,1}(1)$, we need to do subtraction to get $\hat{g}_i(2) - [\hat{r}_{i,2}(0) + \hat{r}_{i,1}(1)] = \hat{r}_{i,0}(2)$.
3) *Step 3:* Multiplying $\hat{r}_{i,0}(2)$ by the CIRV, we obtain the second symbols from paths 0, 1, and 2, or $\hat{r}_{i,0}(2)\frac{\mathbf{h}}{h(0)} = \left[\hat{r}_{i,2}(1)\right]_{l=0}^{2}$. After having acquired $\hat{r}_{i,2}(1)$ and $\hat{r}_{i,1}(2)$, we perform subtraction to get $\hat{g}_i(3) - [\hat{r}_{i,2}(1) + \hat{r}_{i,1}(2)] = \hat{r}_{i,0}(3)$.
4) *Steps 4–7:* According to the sequential order, as shown in Fig. 4, the samples are processed one by one. After having acquired $\hat{r}_{i,2}(n-2)$ and $\hat{r}_{i,1}(n-1)$, where $n = 3, \ldots, 7$, we make a subtraction to get $\hat{g}_i(n) - [\hat{r}_{i,2}(n-2) + \hat{r}_{i,1}(n-1)] = \hat{r}_{i,0}(n)$. Multiplying $\hat{r}_{i,0}(n)$ with the CIRV, we get the nth symbol from path $l\,(l = 0, 1, 2)$, i.e., $\hat{r}_{i,0}(n)\frac{\mathbf{h}}{h(0)} = \left[\hat{r}_{i,l}(n)\right]_{l=0}^{2}$. In this way, we can obtain all the symbols in an OFDM block.
5) *Step 8:* Fill up the CP "gap" with the estimated signal $[\hat{r}_{i,1}(7) + \hat{r}_{i,2}(6), \hat{r}_{i,2}(7)]$, i.e., Step 8(a), or

$$[\hat{r}_i(n)]_{n=0}^{7} = [g_i(n)]_{n=0}^{7} + \Big[\overbrace{\hat{r}_{i,1}(7) + \hat{r}_{i,2}(6), \hat{r}_{i,2}(7)}^{\text{Estimated CP signal}}, 0, \ldots, 0\Big]^T. \tag{12}$$

Note that the calculation of $[\hat{r}_{i,1}(7) + \hat{r}_{i,2}(6), \hat{r}_{i,2}(7)]$ is exactly the process to substitute $L-1=2$ and $M=8$ into (11) or "Calculation 2" described in Fig. 3. At the same time, (12) should be sent to a memory unit, i.e., Step 8(b), since it will serve as a stored feedback signal to cancel the interference to the next block. For this reason, the algorithm is named as SFE.

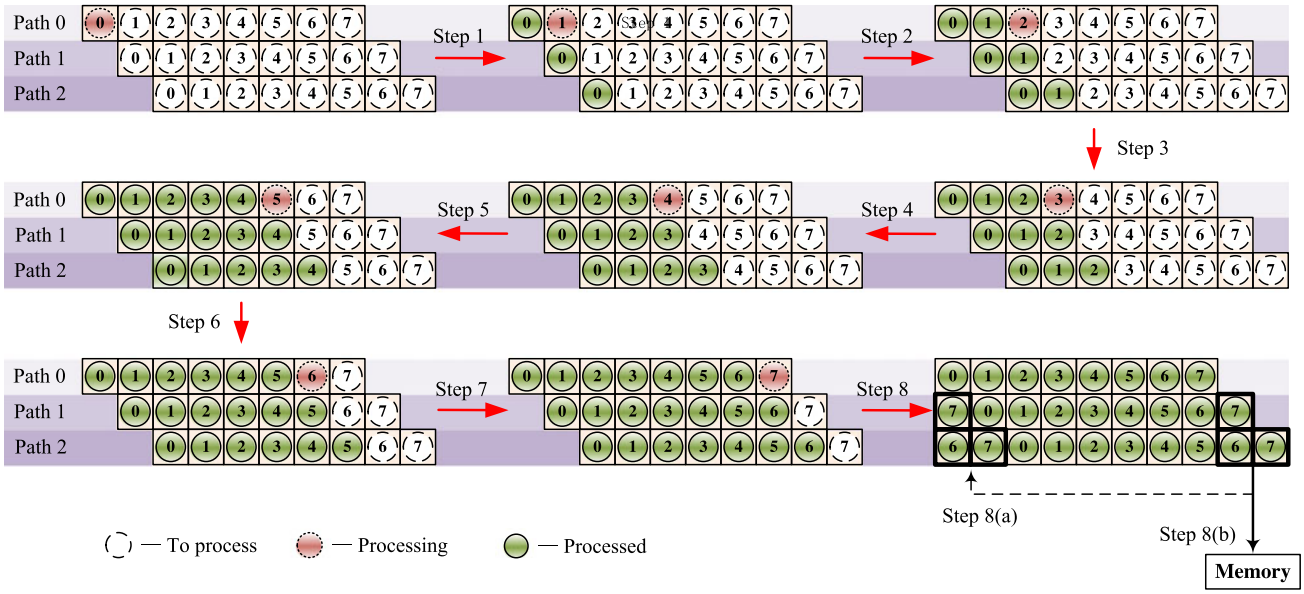

Fig. 4. Schematic diagram of the CPR algorithm, where "ⓝ" refers to the nth symbol in the ith OFDM block.

After Steps 1–8 as introduced above, the CPR algorithm in this example is complete. Note that Step 8 of CPR in this example is very different from the SCSE algorithm [15], [16]. In the SCSE algorithm, DFE uses the recovered block to reconstruct the tail of the previous block and then send it to the current block for ISI cancellation. In the DFE loop, an M-point IFFT and a convolution unit are required, which will significantly complicate the receiver structure and increase computational complexity. In addition, DFE starts from the output of the decision device, and hence, its feedback loop is much longer than

$$
\begin{aligned}
\mathsf{v}_i(0) = {} & \frac{h(1)}{h(0)} w_i(7) - \left[\frac{h^2(1)}{h^2(0)} - \frac{h(2)}{h(0)}\right] w_i(6) + \left[\frac{h^3(1)}{h^3(0)} - \frac{2h(1)h(2)}{h^2(0)}\right] w_i(5) \\
& - \left[\frac{h^4(1)}{h^4(0)} - \frac{3h^2(1)h(2)}{h^3(0)} + \frac{h^2(2)}{h^2(0)}\right] w_i(4) + \left[\frac{h^5(1)}{h^5(0)} - \frac{4h^3(1)h(2)}{h^4(0)} + \frac{3h^2(2)h(1)}{h^3(0)}\right] w_i(3) \\
& - \left[\frac{h^6(1)}{h^6(0)} - \frac{5h^4(1)h(2)}{h^5(0)} + \frac{6h^2(1)h^2(2)}{h^4(0)} - \frac{h^3(2)}{h^3(0)}\right] w_i(2) \\
& + \left[\frac{3h^7(1)}{h^7(0)} - \frac{5h^5(1)h(2)}{h^6(0)} + \frac{4h^3(1)h^2(2)}{h^5(0)} - \frac{h^3(2)h(1)}{h^4(0)}\right] w_i(1) \\
& - \left[\frac{h^8(1)}{h^8(0)} - 4\frac{h^6(1)h(2)}{h^7(0)} + \frac{h^6(1)}{h^6(0)} - 2\frac{h^2(1)h^3(2)}{h^5(0)} + 4\frac{h^4(1)h^2(2)}{h^6(0)} \right. \\
& \left. - \frac{h^4(1)h(2)}{h^5(0)} + \frac{h^2(1)h^2(2)}{h^4(0)}\right] w_i(0) \\
\mathsf{v}_i(1) = {} & \frac{h(2)}{h(0)} w_i(7) - \frac{h(1)h(2)}{h^2(0)} w_i(6) + \left[\frac{h^2(1)h(2)}{h^3(0)} - \frac{h^2(2)}{h^2(0)}\right] w_i(5) \\
& - \left[\frac{h^3(1)h(2)}{h^4(0)} - \frac{2h(1)h^2(2)}{h^3(0)}\right] w_i(4) + \left[\frac{h^4(1)h(2)}{h^5(0)} - \frac{3h^2(1)h^2(2)}{h^4(0)} + \frac{h^3(2)}{h^3(0)}\right] w_i(3) \\
& - \left[\frac{h^5(1)h(2)}{h^6(0)} - \frac{4h^3(1)h^2(2)}{h^5(0)} + \frac{3h^3(2)h(1)}{h^4(0)}\right] w_i(2) \\
& - \left[4\frac{h^4(1)h^2(2)}{h^6(0)} - 3\frac{h^6(1)h(2)}{h^7(0)} - \frac{h^2(1)h^3(2)}{h^5(0)}\right] w_i(1) \\
& - \left[\frac{h^7(1)h(2)}{h^8(0)} - 3\frac{h^5(1)h^2(2)}{h^7(0)} + \frac{h^5(1)h(2)}{h^6(0)} + \frac{h(1)h^4(2)}{h^5(0)}\right] w_i(0)
\end{aligned} \tag{13}
$$

SFE as used in SMIC. The delay caused by a long feedback loop may interrupt signal detection when the feedback signal cannot be acquired immediately. If a channel coding scheme is employed, the decoding will inevitably prolong the feedback delay further. This is a well-known drawback of DFE [22], [23]. To solve this problem, SMIC stores the tail of the current block, which will interfere the next block, at the final step of CPR, and SFE is carried out depending only on a memory unit. Therefore, SFE is more robust than DFE. Without loss of generality, the CPR algorithm as described in this example can be extended to a more general case with the delay spread $L-1$ and the block size M, where $L-1<M$.

As presented in Fig. 4, CPR can turn linearly shifted OFDM blocks into circularly shifted blocks. However, a CPR may bring in estimation errors, which are generated by CPR and defined as $[\mathsf{v}_i(n)]_{n=0}^{L-2}=[\hat{I}_i(n)-I_i(n)]_{n=0}^{L-2}$. To match to the size of an OFDM block, $M-L+1$ zeros are padded at the tail of $[\mathsf{v}_i(n)]_{n=0}^{L-2}$ to form $\mathbf{v}_i=[\mathsf{v}_i(n)]_{n=0}^{M-1}=[\mathsf{v}_i(0),\mathsf{v}_i(1),\ldots,\mathsf{v}_i(L-2),0,\ldots,0]$. In the case as shown in Fig. 4, $\mathbf{v}_i$ can be expressed as $\mathbf{v}_i=[\mathsf{v}_i(0),\mathsf{v}_i(1),0,\ldots,0]$. $\mathsf{v}_i(0)$ and $\mathsf{v}_i(1)$ can be written as (13) shown at the bottom of the previous page, whose derivations are omitted and only the result is given.

After CPR, a newly established OFDM block $\hat{\mathbf{r}}_i=[\hat{r}_i(n)]_{n=0}^{M-1}$ consists of circularly shifted OFDM blocks, which can be expressed as $\hat{\mathbf{r}}_i=\mathcal{H}\mathbf{s}_i+\mathbf{w}_i+\mathbf{v}_i$, in which $\mathcal{H}$ is a circulant matrix, and is given in (14) shown at the bottom of this page.

After SMIC, $\hat{\mathbf{r}}_i$ will be sent to an M-point FFT, and we get

$$\begin{aligned}\bar{\mathbf{q}}_i&=\mathbf{F}\hat{\mathbf{r}}_i=\mathbf{F}\left[\mathcal{H}\mathbf{s}_i+\mathbf{w}_i+\mathbf{v}_i\right]\\&=\mathbf{F}\mathcal{H}\mathbf{F}^{-1}\mathbf{q}_i+\mathbf{F}(\mathbf{w}_i+\mathbf{v}_i)\\&=\mathbf{\Lambda}\mathbf{q}_i+\mathbf{F}(\mathbf{w}_i+\mathbf{v}_i)\end{aligned}\tag{15}$$

where $\mathbf{w}_i$ and $\mathbf{v}_i$ denote noise and estimation errors, respectively. $\mathbf{\Lambda}$ is a diagonal matrix, whose diagonal elements are the frequency responses of the CIR $[h(l)]_{l=0}^{L-1}$ [25]. After P/S, frequency-domain equalization (FDE) is performed to remove the random phases before decision, or

$$\hat{\mathbf{q}}_i^T=\mathbf{\Lambda}^{-1}\bar{\mathbf{q}}_i^T=\mathbf{q}_i^T+\mathbf{\Lambda}^{-1}(\mathbf{w}_i+\mathbf{v}_i)^T\mathbf{F}^T.\tag{16}$$

Finally, $\hat{\mathbf{q}}_i^T$ is sent to a decision device. After that, a demapper turns the recovered data block into the binary outputs $\hat{\mathbf{b}}_i^T$.

IV. Simulation Results and Performance Analysis

Before giving the simulation results, we introduce a channel model and a performance metric first. An exponential decay Rayleigh multipath channel model is used such that the average power of path l is $P_l=\mathrm{E}[||h(l)||^2]=P_0e^{-\alpha l}$ $(l=0,\ldots,L-1)$, where $h(l)$ is the complex gain of path l and α is the interpath power decay factor, which describes the power decay speed of multipath signals with time.

The SMIC algorithm does not require a CP to suppressing ISI/ICI in a multipath scenario, saving the spectrum consumed by the CP in conventional OFDM systems. On one hand, SMIC-OFDM can offer a higher channel utilization ratio (CUR) than traditional CP-OFDM. The CUR is defined as

$$\xi=\begin{cases}1, & \text{CP-free OFDM}\\ \dfrac{M}{M+L-1}, & \text{CP-OFDM}\end{cases}\tag{17}$$

where M and $L-1$ denote the lengths of an original OFDM block and the CP, respectively. Here, the length of the CP is made equal to the delay spread. On the other hand, SMIC may yield estimation errors in its CPR operation, which can be accumulated in SFE, resulting in a poor BER performance. To make a fair comparison, we employ *capacity* as a performance metric in the simulations, which is defined as the CUR multiplied by the Shannon capacity [18], or

$$C=\mathrm{E}\left[\xi B\log_2\left(1+\frac{||\mathbf{q}_i||^2}{||\mathbf{F}(\mathbf{w}_i+\mathbf{v}_i)\mathbf{\Lambda}_i^{-1}||^2}\right)\right]\ \text{(bits/s)}\tag{18}$$

in which "$||\cdot||$," "$\mathrm{E}(\cdot)$," and B denote the Frobenius norm, the expectation of "$\cdot$," and the total bandwidth, respectively.

Fig. 5 is to evaluate the BER and capacity performances for SMIC-OFDM and CP-OFDM with different decay factors, where 16-ary QAM (16QAM) is considered and the bandwidth is $B=100$ MHz. The length of an OFDM/OFDM block is equal to 64, i.e., $M=64$, and the delay spread is $L-1=16$. It can be seen from Fig. 5 that a higher signal-to-noise ratio (SNR) brings in a lower BER and a higher capacity for both CP-OFDM and SMIC-OFDM. Additionally, a smaller α gives a higher BER and a lower capacity, since channel power decay speed is low, and it

$$\mathcal{H}=\begin{bmatrix}h(0) & 0 & \cdots & 0 & h(L-1) & \cdots & h(1)\\ \vdots & \ddots & \ddots & & \ddots & \ddots & \vdots\\ \vdots & & \ddots & \ddots & & \ddots & h(L-1)\\ h(L-1) & & & \ddots & \ddots & & 0\\ \vdots & \ddots & & & \ddots & \ddots & \vdots\\ \vdots & \ddots & \ddots & & & \ddots & 0\\ 0 & \cdots & 0 & h(L-1) & \cdots & \cdots & h(0)\end{bmatrix}_{M\times M}\tag{14}$$

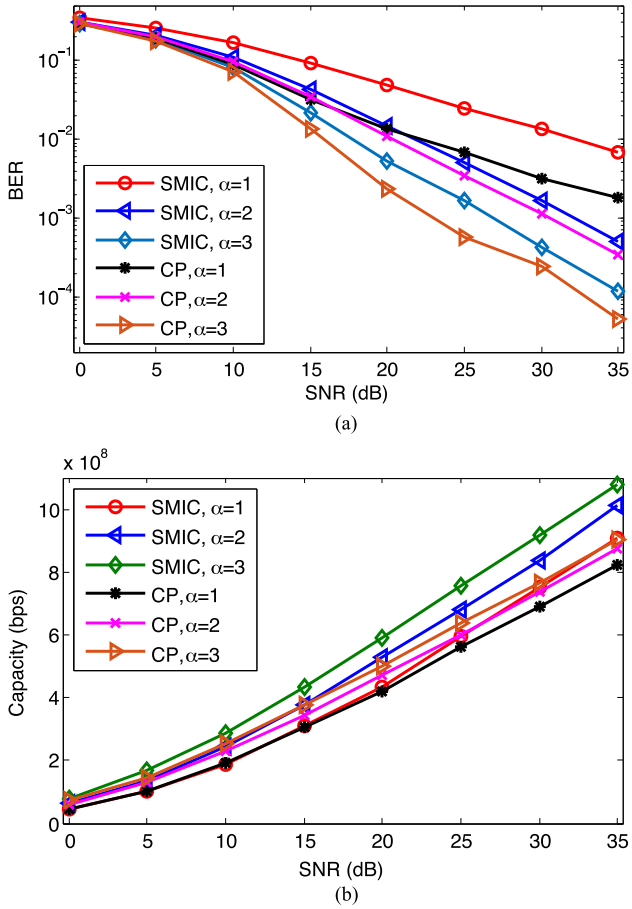

Fig. 5. BERs and capacities of SMIC-OFDM and CP-OFDM with different decay factors, where the bandwidth is 100 MHz, 16QAM modulation is used, the length of an OFDM block is 64, and the delay spread is 16. Here, α refers to the interpath decay factor. (a) Comparisons of BER performances with different interpath decay factors. (b) Comparisons of capacities with different interpath decay factors.

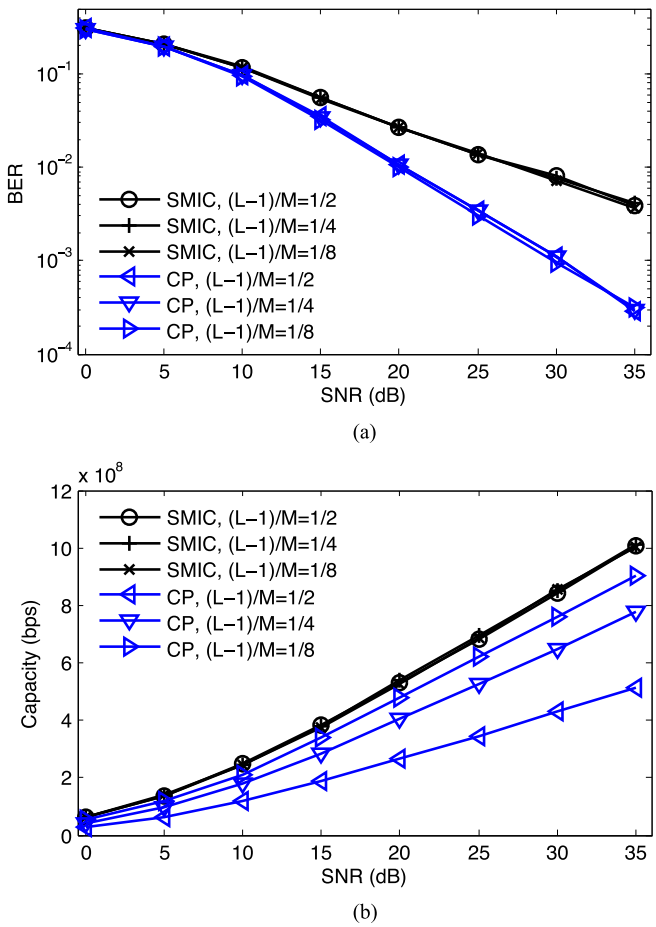

Fig. 6. BER and capacity performances of CP-OFDM and SMIC-OFDM with different delay spreads, where the block length is 16, the interpath decay factor is 1, and 16QAM modulation is used. (a) Comparisons of BER performances with different delay spreads. (b) Comparisons of capacities with different delay spreads.

is more likely to produce a deep fading. We can see from Fig. 5(a) that the BER performance of CP-OFDM is better than that of SMIC-OFDM. As mentioned earlier, CPR will produce estimation error and SFE may cause error propagation, and hence, the BER performances of SMIC-OFDM can be degraded. In a case with a smaller α, the delayed signal is stronger and a larger estimation error will occur, since the gains of delayed paths appear in the numerator of the estimation error term, as shown in (13). It is indicated in Fig. 5(b) that the decay factor α has a more significant impact to SMIC-OFDM than that to CP-OFDM. For example, under SNR = 30 dB, the capacity gap for the CP-based scheme with $\alpha = 1$ to $\alpha = 3$ is about 1×10^8 bits/s; while the gap for SMIC is more than 2×10^8 bits/s. The reason can be explained from (13) and (18). It is also observed that in most of the cases, the SMIC scheme achieves a higher capacity than the CP-based scheme. As introduced in Section III, SMIC-OFDM combats multipath interference by the SMIC algorithm without CP insertion in an OFDM block, and the spectrum is utilized more efficiently than a CP-OFDM system.

In Fig. 6, we show BER and capacity performances with different delay spreads. The simulations used relative delay spread, that is defined as $(L-1)/M$, as a parameter, which is $1/8$, $1/4$, and $1/2$, respectively. We consider 16QAM modulation, and the interpath decay factor is $\alpha = 1$. The bandwidth is 100 MHz. Let the CP length be equal to delay spread. It can be easily observed from Fig. 6(a) that the BER performance of the SMIC-OFDM is worse than that of CP-OFDM, since the CPR produces estimation errors, which will propagate to the following OFDM blocks, thus deteriorating the BER of the SMIC scheme. In addition, with the same SNR, it can be seen that BERs of SMIC-OFDM and CP-OFDM keep almost unchanged with $(L-1)/M$. In CP-OFDM, the increase of $(L-1)/M$ requires a longer CP insertion between OFDM blocks to overcome ISI/ICI, leading to a worse spectrum efficiency, while in SMIC-OFDM, it will require more complex computations to resist against ISI/ICI with increasing $(L-1)/M$. Fig. 6(b) shows that the capacity of SMIC-OFDM is almost constant as $(L-1)/M$ increases, while the capacity of CP-OFDM will be reduced significantly, as a larger $(L-1)/M$ gives a smaller CUR, i.e., ξ, as shown in (17).

The simulations given in Fig. 7 evaluate the BER of SMIC-OFDM with different modulations. In the simulations, the bandwidth is assumed to be 100 MHz, the interpath decay factor is $\alpha = 1$, the number of subcarriers is 64, and the delay spread is

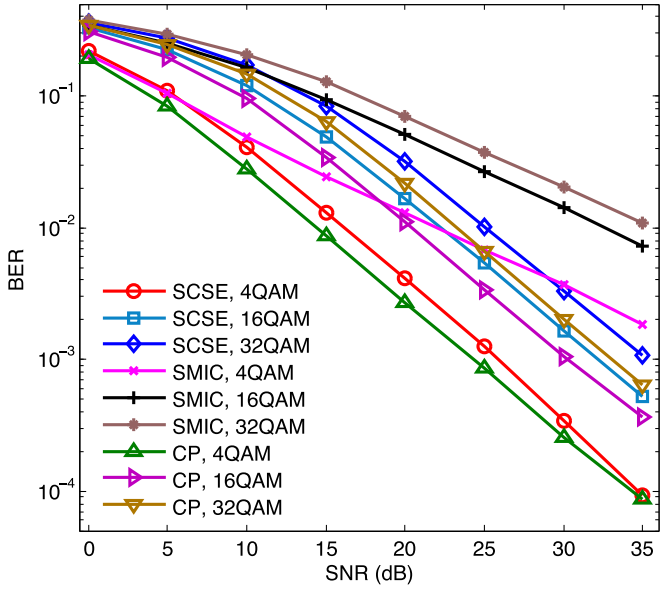

Fig. 7. BER comparisons among SCSE, SMIC, and CP schemes with different modulations, where the interpath decay factor α is equal to 1.

16. It is easy to see that a higher modulation level gives a higher BER under the same SNR. According to the curves shown in Fig. 7, if different modulations are sorted from good to poor relevant to the BER performance, we have 4, 16, and 32QAM. CP-OFDM has the best BER if the comparisons are made among CP, SMIC, and SCSE schemes. Due to the overhead of the CP, the CUR of CP-OFDM is only $\xi = 4/5$, as shown in (17). Fig. 7 also shows that the BER of SCSE is better than SMIC. This is because, in the SMIC algorithm, owing to noise, the CPR algorithm will produce estimation errors, which will be saved in memory. In the next detection cycle, the SFE brings the estimation errors from the memory into detection, resulting in an accumulation effect. The SCSE algorithm uses DFE to eliminate ISI, while DFE reconstructs the ISI term using the data after decision. The data output from a decision device generally does not contain noise. The feedback error caused by DFE is a Markov process because the feedback error in the current detection cycle is only affected by the symbol error rate in the previous detection cycle. Therefore, in the SCSE algorithm, the estimation error in CPR will not be accumulated. From the viewpoint of the BER, DFE is better than SFE; however, the complexity of DFE is high, and it is likely to have a long feedback delay, especially when the channel coding is used. Therefore, in terms of delay performance, SFE is better than DFE.

In Fig. 8, the simulation results are given to evaluate the BER and the capacity of SMIC-OFDM in 3GPP-LTE channel models, which includes an extended vehicle A (EVA) channel and an extended typical urban (ETU) channel. The delay profiles of EVA and ETU channel models can be found in [4]. The bandwidth is 10 MHz, and the number of subcarriers is 64. The delay spreads of EVA and ETU channels are 2510 and 5000 ns, respectively. At a symbol rate of 10 Mbaud/s, the number of distinguishable paths of EVA and ETU channel models is seven. Let the length of the CP be equal to the delay spread for CP-OFDM, where the modulation is 16QAM. It can be seen

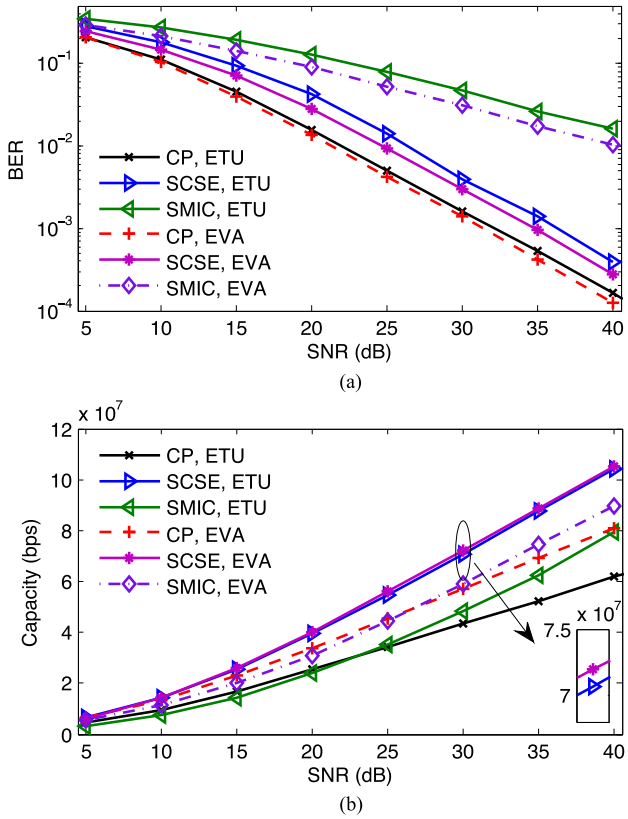

Fig. 8. BER performances and capacities of CP-OFDM, SMIC-OFDM, and SCSE-OFDM in EVA and ETU channel models. SCSE-OFDM was proposed in our earlier works presented in [15]. (a) BER comparisons among CP, SCSE, and SMIC schemes. (b) Capacity comparisons among CP, SCSE, and SMIC schemes.

from Fig. 8(a) that the BER performance of the CP-based scheme is better than that of SCSE and SMIC schemes, and SMIC has the worst BER. In SCSE-OFDM, CPR may cause estimation error(s), and DFE may cause feedback error(s). Thus, the BER is not as good as CP-OFDM. For SMIC-OFDM, due to the estimation error caused by CPR, SFE will accumulate estimation error, resulting in a more serious error propagation problem, which deteriorates its BER. In addition, it can be observed from Fig. 8(b) that the capacity of SCSE-OFDM is significantly better than that of SMIC-OFDM and CP-OFDM. For SMIC, the estimation error caused by CPR makes a larger variance of $\mathbf{v}_i$ in (18), resulting in a relatively low capacity. Also, as shown in (18), one of the main factors governing the capacity is CUR, i.e., ξ. Since the CP is inserted into an OFDM symbol, CUR will become relatively small, and hence, the capacity of CP-OFDM is significantly lower than that of SCSE-OFDM. In a low-SNR region, the SMIC-OFDM capacity is lower than that of CP-OFDM because the dominant factor is SNR. However, as the SNR increases, the SMIC-OFDM capacity will be higher than CP-OFDM. The reason is that CPR brings in much less estimation error under a high SNR, and CUR plays a dominant role in capacity performance.

Fig. 9 evaluates the computational complexity of the SMIC algorithm, where we used the number of complex multiplications as a computational complexity metric. RISIC

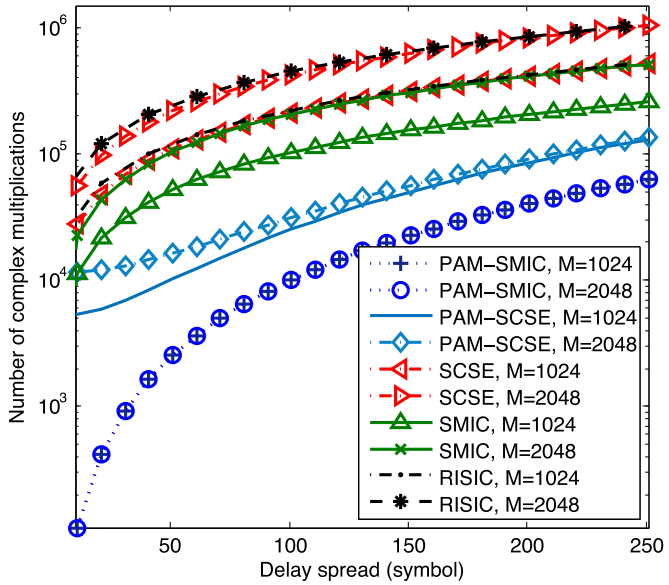

Fig. 9. Computational complexity of the SMIC algorithm in SCSE, PAM-SCSE, and RISIC schemes, which were proposed in [15], [16], and [8], respectively. Here, M stands for the length of an OFDM block.

is a CP-free scheme, whose computational complexity is [8]

$$O_{\text{RISIC}} = (o+1)\,ML + \frac{2o+1}{2}\log_2 M + oM \tag{19}$$

in which o refers to the iteration times. M and $L-1$ stand for the block length and the delay spread, respectively. SCSE is our earlier proposed scheme [15], in which we also discussed the computational complexity. For the implementation of the SCSE algorithm, DFE is required to cancel ISI, which consists of an IFFT and a convolution operation. Considering the base-2 Cooley–Tukey FFT/IFFT algorithm, we can calculate the complexity of IFFT as $M\log_2 M/2$, and the complexity of convolution operation is ML[24]. Then, the complexity of CPR in an SCSE scheme is ML, which takes all samples in an OFDM block into calculations, and this is the main difference from PAM-CPR proposed in [16]. For one block detection, a PAM-CPR will require $L(L-1)$ complex multiplications. For the implementation of the SMIC algorithm, SFE that performs $[\hat{r}_i(n) - \hat{I}_{i-1}(n)]_{n=0}^{L-2} = [\hat{g}_i(n)]_{n=0}^{L-2}$ consumes $L-1$ complex additions without any complex multiplications. The calculation of $[\hat{r}_{i,0}(n)\frac{\mathbf{h}}{h(0)}]_{n=0}^{L-2}$ in CPR costs ML complex multiplications. Therefore, to detect one block data, the complexity of the SMIC algorithm is ML. Also, if PAM is used in an SMIC-OFDM transmitter, we can use PAM-CPR and SFE to construct PAM-SMIC. The details about PAM-CPR can be found in our earlier work [16]. As shown in Fig. 9, PAM-SMIC has the lowest complexity among three CP-free schemes, while RISIC has the highest computational complexity. Moreover, the complexity of SCSE, RISIC, and SMIC depends more heavily on the block length than PAM-SMIC. However, it is noted that PAM-SMIC enjoys a significantly reduced complexity only under the condition that PAM modulation is used in a transmitter to construct conjugation symmetrical OFDM blocks [16].

V. Conclusion

This work proposed a CP-free OFDM system together with an interference cancellation algorithm named as SMIC. Different from our earlier effort, i.e., SCSE algorithm, SMIC utilizes SFE to combat ISI, and the implementation of SFE is much easier than DFE used in SCSE. Additionally, the feedback loop of SFE is much shorter than DFE, and thus, SFE is effective to reduce feedback delays. Also, since a CP is not required in signal transmission, the simulations verified that the proposed SMIC-OFDM can achieve a significantly higher capacity than traditional CP-based OFDM but with a loss in BER due to estimation errors in CPR. Looking for a way to deal with the estimation errors for SMIC-OFDM will be one of the most important future works. Without using a CP in SMIC-OFDM, the duration of an OFDM block can also be made much shorter without any loss in the spectrum efficiency. Therefore, SMIC-OFDM is particularly suitable for the applications that need to send short packets, such as an all-IP wireless system.

References

[1] E. Dahlman, S. Parkvall, and J. Skold, *4G: LTE/LTE-Advanced for Mobile Broadband*. San Francisco, CA, USA: Academic, 2013.
[2] Y. G. Li and G. L. Stuber, *Orthogonal Frequency Division Multiplexing for Wireless Communications*. New York, NY, USA: Springer, 2006.
[3] E. Lähetkangas *et al.*, "On the selection of guard period and cyclic prefix for beyond 4G TDD radio access network," in *Proc. 19th Eur. Wireless Conf.*, 2013, pp. 1–5.
[4] E. LTE, "Evolved universal terrestrial radio access (E-UTRA); Base station (BS) radio transmission and reception (3GPP TS 36.104 Version 12.6. 0 Release 12)," *ETSI TS*, vol. 136, no. 104, pp. 128–141, 2015.
[5] A. A. Al-Jzari and I. Kostanic, "Effect of variable cyclic prefix length on OFDM system performance over different wireless channel models," *Universal J. Commun. Netw.*, vol. 3, no. 1, pp. 7–14, 2015.
[6] G. Durisi, T. Koch, and P. Popovski, "Toward massive, ultrareliable, and low-latency wireless communication with short packets," *Proc. IEEE*, vol. 104, no. 9, pp. 1711–1726, Sep. 2016.
[7] C. J. Park and G. H. Im, "Efficient DMT/OFDM transmission with insufficient cyclic prefix," *IEEE Commun. Lett.*, vol. 8, no. 9, pp. 576–578, Sep. 2004.
[8] D. Kim and G. L. Stuber, "Residual ISI cancellation for OFDM with applications to HDTV broadcasting," *IEEE J. Sel. Areas Commun.*, vol. 16, no. 8, pp. 1590–1599, Oct. 1998.
[9] Z. Yang, W. Bai, and Z. Liu, "A decision-aided residual ISI cancellation algorithm for OFDM systems," in *Proc. 8th Int. Conf. Signal Process.*, 2006, vol. 3, pp. 16–20.
[10] H. M. Kim, D. Kim, G.-H. Im, and S. Ahn, "Subband interference suppression in channel shortening for OFDMA downlink systems," in *Proc. IEEE Wireless Commun. Netw. Conf.*, 2013, pp. 3726–3731.
[11] P. J. Melsa, R. C. Younce, and C. E. Rohrs, "Impulse response shortening for discrete multitone transceivers," *IEEE Trans. Commun.*, vol. 44, no. 12, pp. 1662–1672, Dec. 1996.
[12] K. Shimezawa, T. Yoshimoto, R. Yamada, N. Okamoto, and K. Imamura, "A novel SC/MMSE turbo equalization for multicarrier systems with insufficient cyclic prefix," in *Proc. IEEE 19th Int. Symp. Pers., Indoor Mobile Radio Commun.*, 2008, pp. 1–5.
[13] K. Anwar, Z. Hui, and T. Matsumoto, "Chained turbo equalization for block transmission without guard interval," in *Proc. IEEE 71st Veh. Technol. Conf.*, 2010, pp. 1–5.
[14] B. Muquet, P. Magniez, P. Duhamel, M. de Courville, and G. Giannakis, "Turbo demodulation of zero-padded OFDM transmissions," in *Proc. Conf. Rec. 34th Asilomar Conf. Signals, Syst., Comput.*, 2000, vol. 2, pp. 1815–1819.
[15] X. Liu, H. H. Chen, S. Chen, and W. Meng, "Symbol cyclic-shift equalization algorithm—A CP-free OFDM system design," *IEEE Trans. Veh. Technol.*, vol. 66, no. 1, pp. 282–294, Jan. 2017.
[16] X. Q. Liu, H. H. Chen, B. Y. Lyu, and W. X. Meng, "Symbol cyclic shift equalization PAM-OFDM—A low complexity CP-free OFDM scheme," *IEEE Trans. Veh. Technol.*, vol. 66, no. 7, pp. 5933–5946, Jul. 2017.

[17] C. Y. Ma, S. W. Liu, and C. C. Huang, "Low-complexity ICI suppression methods utilizing cyclic prefix for OFDM systems in high-mobility fading channels," *IEEE Trans. Veh. Technol.*, vol. 63, no. 2, pp. 718–730, Feb. 2014.
[18] C. E. Shannon, "A mathematical theory of communication," *Bell Syst. Tech. J.*, vol. 27, no. 3, pp. 379–423, Jul. 1948.
[19] H. N. Kim, S. I. Park, and S. W. Kim, "Performance analysis of error propagation effects in the DFE for ATSC DTV receivers," *IEEE Trans. Broadcast.*, vol. 49, no. 3, pp. 249–257, Sep. 2003.
[20] R. L. Kosut, W. Chung, C. Johnson, and S. P. Boyd, "On achieving reduced error propagation sensitivity in DFE design via convex optimization," in *Proc. 39th IEEE Conf. Decision Control*, 2000, vol. 5, pp. 4320–4323.
[21] M. Ghosh, "Analysis of the MMSE-DFE with error propagation," in *Proc. IEEE GLOBECOM*, 1997, pp. 85–89.
[22] Y. Gong and C. F. Cowan, "Optimum decision delay of the finite-length DFE," *IEEE Signal Process. Lett.*, vol. 11, no. 11, pp. 858–861, Nov. 2004.
[23] A. Goldsmith, *Wireless Communications*. Cambridge, U.K.: Cambridge Univ. Press, 2005.
[24] R. G. Lyons, *Understanding Digital Signal Processing*, 3rd ed. Englewood Cliffs, NJ, USA: Prentice-Hall, 2010.
[25] R. M. Gray *et al.*, "Toeplitz and circulant matrices: A review," *Found. Trends Commun. Inf. Theory*, vol. 2, no. 3, pp. 155–239, 2006.
[26] Z. Ding, "Multipath channel identification based on partial system information," *IEEE Trans. Signal Process.*, vol. 45, no. 1, pp. 235–240, Jan. 1997.

Xiqing Liu received the M.Sc. degree from the Harbin University of Science and Technology, Harbin, China, in 2012, and the Ph.D. degree from the Harbin Institute of Technology, Harbin, in 2017.

He is currently a Postdoctoral Fellow with the Department of Engineering Science, National Cheng Kung University, Tainan, Taiwan. His current research interests include interference suppression algorithms in cyclic-prefix-free orthogonal frequency-division multiplexing/orthogonal frequency-division multiple-access systems, complementary code code-division multiple-access technology, and physical layer security in intelligent connected vehicles.

Hsiao-Hwa Chen (S'89–M'91–SM'00–F'10) received the B.Sc. and M.Sc. degrees in electrical engineering from Zhejiang University, Hangzhou, China, in 1982 and 1985, respectively, and the Ph.D. degree in electrical engineering from the University of Oulu, Oulu, Finland, in 1991.

He is currently a Distinguished Professor with the Department of Engineering Science, National Cheng Kung University, Tainan, Taiwan.

Dr. Chen is the founding Editor-in-Chief of Wiley's *Security and Communication Networks Journal*. He is the recipient of 2016 IEEE Jack Neubauer Memorial Award. He was the Editor-in-Chief for IEEE WIRELESS COMMUNICATIONS from 2012 to 2015. He was an Elected Member-at-Large of the IEEE Communications Society from 2015 to 2017. He is a Fellow of the Institution of Engineering and Technology.

Weixiao Meng (M'02–SM'10) received the B.Eng., M.Eng., and Ph.D. degrees in information and communication engineering from the Harbin Institute of Technology (HIT), Harbin, China, in 1990, 1995, and 2000, respectively.

He is currently a Full Professor with the School of Electronics and Information Engineering, HIT. His research interests include broadband wireless communications and networking, multi-input and multi-output, global navigation satellite system receiver, and wireless localization technologies.

Dr. Meng is the Chair of the IEEE Communications Society Harbin Chapter and a senior member of the China Institute of Electronics and the China Institute of Communications.

Bo-Yu Lyu received the B.Sc. and M.Sc. degrees in communication and information engineering from the School of Electronics and Information Engineering, Harbin Institute of Technology, Harbin, China, in 2015 and 2017, respectively. He is currently working toward the Ph.D. degree with the Bradley Department of Electrical and Computer Engineering, Virginia Polytechnic Institute and State University, Blacksburg, VA, USA.

His current research interests include machine learning, deep learning, and genomics data analysis.